RSC Advances




ROYAL SOCIETY OF CHEMISTRY

www.rsc.org/advances

# Magnetic Electrochemical Immunosensor for Detection of Phosphorylated p53 based on Enzyme Functionalized Carbon Nanospheres as Signal Amplification

Yanan Luo,[a] Abdullah Mohamed Asiri,[b] Xiao Zhang,[a] Guohai Yang,[c] Dan Du,[a,c,*] Yuehe Lin [b,c,*]

[a] *Key Laboratory of Pesticide and Chemical Biology of Ministry of Education, College of Chemistry, Central China Normal University, Wuhan 430079, PR China*

[b] *Chemistry Department, King Abdulaziz University, Jeddah 21589, Saudi Arabia*

[c] *School of Mechanical and Materials Engineering, Washington State University, Pullman, WA 99164, USA*

* Corresponding authors. Email: dan.du@mail.ccnu.edu.cn or yuehe.lin@wsu.edu

***Abstract***

Protein phosphorylation plays an important role in many biological processes and might be used as a potential biomarker in clinical diagnoses. We reported the development of a nanomaterial enhanced disposable immunosensor for ultrasensitive detection of phosphorylated p53 at Ser392 (phospho-p53$^{392}$) using enzyme functionalization of carbon nanospheres (CNSs) as a signal amplification label and magnetic beads (MB) coupled with screen printed carbon electrodes as electrochemical transducers. In this work, horseradish peroxidase (HRP) and phospho-p53$^{392}$ detection antibody ($Ab_2$) were co-linked to CNSs (HRP-CNSs-$Ab_2$) for signal amplification, and functionalized MB was used as platform to capture a large amount of primary antibodies ($Ab_1$). The proposed signal amplification strategy with a sandwich-type immunoreaction significantly enhanced the sensitivity of detection of biomarkers. Under optimal conditions, the immunosensor had a highly linear voltammetric response to the phospho-p53$^{392}$ concentration in the range of 0.01 to 5 ng/mL, with a detection limit of 3.3 pg/mL. The results provided great potential for point-of-care detection of other phosphorylated proteins and clinical applications.

*Keywords:* Electrochemical Immunoassay; Carbon Nanospheres; Magnetic Beads; Phosphorylated p53$^{392}$; Signal Amplification

## 1. Introduction

The p53 protein is a sequence-specific transcription factor that has a significant role in human cancer. Its functions involved in cell cycle arrest, DNA repair, and/or apoptosis, and represses transcriptional activation of growth-promoting genes [1-3]. For half of all human cancer cases, the p53 gene contains mutations that disrupt p53 protein function [4,5]; most of these are missense mutations within the DNA-binding domain that result in altered conformation and decreased DNA binding. p53 is multiply phosphorylated at serine and threonine within its amino- and carboxy-terminal regions in vivo and in vitro [6,7]. Studies show that phosphorylation of C-terminal S392 may be involved in the cell's response to UV exposure [8,9]. Therefore, establish a sensitive and accurate method for early detection of phosphorylated p53 is significant to medical diagnosis and treatments.

Up to now, the conventional method for measuring phosphorylated p53 is enzyme-linked immunosorant assay (ELLSA) [10-12]. Although ELISA is a powerful tool for the detection of antigens and several commercial detection kits are available, it involves several incubation and washing steps followed by spectrophotometric detection using a chromogenic substrate. In addition, ELISA needs more expensive instruments and is lab oriented. A simple, sensitive, and reliable immunoassay for detection of phosphorylated proteins is urgently needed. Electrochemical immunoassay has gained growing attention since they combined the high specificity of traditional immunoassay methods with low detection limits and low expenses of electrochemical measurement system [13-15]. In order to improve the sensitivity and selectivity of the immunosensors, various nanomaterials have been used either as promoters to increase the surface area and improve the electron transfer [16-18] or as carriers to load a large amount of signal molecules and enhance signal responses. The applications of gold nanoparticles [19], silica nanoparticles [20], and carbon-based nanomaterials [21-27], etc. have been widely reported for this purpose. One of the most popular strategies is

enzyme-functionalized nanoparticles used as labels to enhance the detection sensitivity by loading a large amount of enzyme toward an individual sandwich immunological reaction event. For example, Rusling's group [28,29] has achieved greatly enhanced sensitivity using bioconjugates featuring horseradish peroxidase (HRP) labels and signal antibodies linked to carbon nanotubes for immunodetection of the prostate-specific antigen and interleukin-6, respectively. Our group has reported using functionalized graphene oxide as a nanocarrier in a multienzyme labeling amplification strategy for ultrasensitive electrochemical immunoassay of phosphorylated proteins [30]. Recently, highly porous carbon spheres (CNSs) from networked sugars were synthesized and characterized and have been used as nanocarriers for antibody and enzyme co-immobilization [31-33].

Magnetic beads (MBs) are of increasing interest because of their specific magnetic properties and low toxicity and found to have several biomedical applications [34,35], including bioseparation [36], targeted delivery [37] and stem cell labeling [38]. MBs have been used as sensing platform because of their inherent advantages such as good stability, versatility in chemical modification, and ease of separation. Coupling of MBs with highly sensitive electrochemical detection may provide a useful diagnostics method.

By combining a disposable sensor with functional materials, this paper described an electrochemical immunosensor for detection of phospho-p53$^{392}$ using MBs served as an immobilization scaffold for antibodies, while a multi-enzymes labeling CNSs as the tag. The MBs not only separated the immunocomplex from biological samples under magnetic field, but also provided a large surface to load capture antibody ($Ab_1$). CNSs were used as the nanocarrier to load HRP and detection antibody ($Ab_2$). Coupled with a portable electrochemical analyzer, this method shows great promise for application in biomedical research, clinical diagnosis, and screening exposure biomarkers.

## 2. Experimental

*2.1. Reagents and chemicals*

The Human phospho-p53$^{392}$ ELISA kit including phospho-p53$^{392}$ capture antibody ($Ab_1$), phospho-p53$^{392}$ antigen, biotinylated phospho-p53$^{392}$ detection antibody ($Ab_2$) and streptavidin-HRP were supplied by DuoSet® IC from R&D System, Inc. Bovine serum albumin (BSA), Tween-20, 1-ethyl-3-(3-dimethylaminopropyl) carbodiimide hydrochloride (EDC), N-hydroxysuccinimide (NHS), phosphate buffer saline (PBS), thionine, $H_2O_2$, and 2-(N-morpholino) ethanesulfonic acid (MES) were acquired from Sigma-Aldrich. Paramagnetic microbeads coated with carboxyl groups (particle size: 1.0-2.0 μm) were purchased from Tianjin BaseLine ChroTech Research Centre (China). Blocking solution was 1% (w/v) BSA in 0.01 M pH 7.4 PBS.

*2.2. Instruments*

Transmission electron microscopy (TEM) images were collected with holey carbon TEM grids on a JEOL JSM-2010 TEM microscope operated at 200 kV. X-ray photoelectron spectroscopy (XPS) measurements were taken with a Physical Electronics Quantum 2000 scanning microprobe. UV-vis measurements were carried out at room temperature on a Safire 2 microplate reader (Tecan, Switzerland). Fourier transform infrared spectroscopy (FT-IR) was performed on a Nicolet 6700 spectrometer (Nicolet, USA). Electrochemical experiments, including cyclic voltammetry (CV) and square wave voltammetry (SWV), were performed with an electrochemical analyzer CHI 660C electrochemical analyzer (Shanghai, China) connected to a personal computer. Disposable screen-printed carbon electrodes (SPCE) including a carbon counter electrode and an Ag/AgCl reference electrode were purchased from Alderon Biosciences, Inc.

*2.3. Conjugation of $Ab_1$ with magnetic beads*

Briefly, 100 μL of 10 mg mL$^{-1}$ carboxylated magnetic beads (MBs) was initially sonicated for 5 min, and then washed 5 times with pH 7.4 PBS. The carboxylated MBs were dispersed

in 1.0 mL pH 7.4 PBS. To attach $Ab_1$, the dispersion was mixed with 1.0 mL of 400 mM EDC and 100 mM NHS in pH 5.2 MES and vortexed for 60 min. The resulting mixture was washed with pH 7.4 PBS to remove excessive EDC and NHS. The final volume was set 900 μL and vortexed to obtain a homogeneous dispersion. Then, 100 uL of 7.5 μg/mL $Ab_1$ was added to the activated MBs and the mixture was incubated for 12 h at 4 °C. After the incubation, the resulting mixture $Ab_1$-MBs was washed with pH 7.4 PBS several times and re-dispersed in 1.0 mL pH 7.4 PBS containing 3% BSA and stored at 4 °C.

*2.4. Synthesis of Colloidal CNSs*

Colloidal CNSs was synthesized from fructose in closed systems under hydrothermal conditions. Detail synthesis procedure and characterization of the CNSs have been reported previously [31,32]. Briefly, in situ Raman spectra to follow the initial dehydration of fructose to hydrothermal furaldehyde in a concentrated aqueous solution (2.5 M) were measured in real time in a pressurized optical cell (25 mL) at temperatures ranging from 120 to 140 $^{o}$C. A 777.8 nm excitation wavelength was used that effectively suppressed fluorescence from the solution as it began to turn yellow. Measured peak intensities were normalized with respect to the intensity of the incident probe laser. Spectra of 13C NMR were collected from a Chemagenetics spectrometer (500 MHz: solution) and a Chemagenetics spectrometer (300 MHz: solid). The samples were prepared by hydrothermal treatment of the solution in a steel cell at a specific temperature and for a specific time, and then, the reactions were quenched by lowering the temperature naturally.

*2.5. Preparation of HRP-CNSs-$Ab_2$ Conjugation*

First, 10 mg of CNSs was sonicated in a mixtrure solution containing $H_2SO_4$, $HNO_3$, and distilled water (3:1:6, v/v) for 2 h at room temperature, and then the mixture was washed repeatedly with water until pH was about 7.0. Through the step, the surface of CNSs generated carboxylated groups. Second, the carboxylated CNSs was added into 1.0 mL of

400 mM EDC and 100 mM NHS in pH 5.2 MES, and sonicated for 30 min. The mixture was centrifuged for 5 min at 13000 rpm and discarded the supernatant. Third, the 100 μL of 5 μg/mL $Ab_2$ and 100 μL of 1 mg/mL HRP were added to the mixture and stirred for 24 h at room temperature. The mixture was washed with PBS several times to remove unbound HRP and $Ab_2$. Finally, the particles was dispersed in 1.0 mL of pH 7.4 PBS containing 3% BSA and stored at 4 °C for later experiments. The procedure was shown in Scheme 1.

*2.6. Electrochemical Measurements*

Before modification, the SPCE was applied a potential of + 1.2 V under stirring in pH 5.0 acetate buffer for 300 s and then scanned from +0.3 V to +1.1 V and +0.3 V to -1.1 V until a steady-state current-voltage curve was obtained. (1) 10 μL of $Ab_1$-MBs were placed onto the working electrode of the SPCE with an external magnet. (2) 10 μL phospho-p53$^{392}$ of various concentrations were introduced onto the modified electrode and incubated for 50 min, followed by washing with 0.05% Tween-20 and PBS buffer with an external magnetic field. (3) 10 μL HRP-CNSs-$Ab_2$ was added and incubated for 50 min, followed by washing with 0.05% Tween-20 and PBS with an external magnetic field. (4) Electrochemical measurement was recorded in PBS containing 25 μM thionine and 4 mM $H_2O_2$.

**3. Results and Discussion**

*3.1. Signal Amplification Based on MBs and $Ab_2$-CNSs-HRP*

The sandwich immunoassay for phospho-p53$^{392}$ was outlined in Scheme 1, including the signal amplification strategy using multienzyme-antibody labels (A) and traditional labeled protocol (B) on $Ab_1$-MBs. It was noted that MBs not only acted as the platform to increase the surface area that facilitate to capture a mass of $Ab_1$, but also could capture the target to concentrate them together with the assistance of an external magnet. To achieve an amplification signal, a multi-enzyme labeling strategy (A) was adopted instead of a single-enzyme label during the immunoassay (B). Upon the completion of sandwich

immunoreactions, the HRP-CNSs-$Ab_2$ conjugation was introduced onto the electrode surface. Electrochemical detection of enzymatic products is performed in the presence of $H_2O_2$ and thionine. Since the CNSs nanocarriers loaded a large number of HRP, which resulted in greatly enhanced signal.

*3.2. Characterization of Antibody Modified Magnetic Beads*

Figure 1A showed the TEM image of MBs. It demonstrated that MBs were mono-dispersed with the size around 200 nm in diameter (Figure 1B). The uniform MB dispersion was vital for conjugation with $Ab_1$. EDC and NHS agents were used to activate carboxyl groups on MBs. The conjugation of $Ab_1$ and carboxylated MBs was achieved through formation of amide bond between the $NH_2$ groups of antibodies and the COOH of MBs. In order to confirm that the MBs have been labeled with $Ab_1$, FT-IR spectroscopy was used to evaluate the surface modification of MBs. Figure 1C showed the IR absorbance spectra of carboxyl MBs (curve a) and $Ab_1$-MBs (curve b). For the carboxyl MBs, The band at 1700 $cm^{-1}$ was associated with stretching of the C=O bond of carboxyl groups. Deformation of the O-H band was observed at the band of 1480 $cm^{-1}$. The peak at 1320 $cm^{-1}$ was attributed to stretching vibration of the C-O. The vibrational band around 3300 $cm^{-1}$ was assigned to O-H. The FTIR spectrum of $Ab_1$-MB differing from that of MBs by the weakening of the peak at 1680 $cm^{-1}$ suggested the reaction between $NH_2$ and COOH. Therefore C=O was shifted to lower wave number. In addition, there were prominent absorbance peaks at 1520 and 1440 $cm^{-1}$ that are specific to amide I and amide II. FTIR confirmed the successful conjugation of $Ab_1$-MBs. UV-vis was further used to investigate the formation of $Ab_1$-MBs, as shown in Figure 1D. It can be seen that no absorption peak was observed on MBs (curve a), while an obvious absorption peak appeared at 281 nm on $Ab_1$-MBs (curve b). This peak is the same absorption with $Ab_1$ (curve c), indicating the successful binding of $Ab_1$ to MBs.

*3.3. Characterization of the CNSs Conjugate*

In our strategy, CNSs were first generated with carboxyl group using acid treated. In order to facilitate the binding of enzymes and antibodies to CNSs, the carboxylated CNSs were activated through EDC/NHS. Figure 2A displayed UV-vis spectroscopy of HRP, pure phopho-p53$^{392}$Ab$_2$, and the HRP-CNSs-Ab$_2$ conjugate. HRP and Ab$_2$ showed the absorption peaks at 406 nm (curve a) and 280 nm (curve b), respectively. However, after the Ab$_2$ and HRP were bound to CNSs, two obvious absorption peaks were observed (curve c), indicating that Ab$_2$ and HRP were successfully immobilized onto the surface of CNSs.

XPS spectra were further explored to provide solid evidence of the formation of HRP-CNSs-Ab$_2$ conjugate. As shown in Figure 2B, HRP-CNSs-Ab$_2$ (curve a) showed a strong $N_{1s}$ binding energy at 399.9 eV, which was attributed to a typical binding energy of amide nitrogen atoms (HN-C=O). However, no signal was observed on CNSs (curve b). All results above indicated the successful modification of CNSs and the formation of HRP-CNSs-Ab$_2$ conjugate.

*3.4. Electrochemical Behaviors of Immunosensors*

As shown in Figure 3, the cyclic voltammogram did not display any detectable signal on Ab$_1$-MB/SPCE in pH 7.4 PBS (curve a). Upon adding thionine and $H_2O_2$, it exhibited a couple of stable and well-defined redox peaks at -0.248 and -0.289 V (curve b), which correspond to the electrochemical response of thionine. When incubating the immnuosensor with 0.5 ng/mL phospho-p53$^{392}$, no obvious change in signal was observed (data not shown). However, after incubating with HRP-Ab$_2$ solution, the reduction current obviously increased on HRP-Ab$_2$/phospho-p53$^{392}$/Ab$_1$-MB/SPCE (curve c) due to the catalysis of the immobilized HRP toward the reduction of $H_2O_2$. Moreover, when replacing HRP-Ab$_2$ with HRP-CNSs-Ab$_2$ as detection antibody, the electrocatalytic current at HRP-CNSs-Ab$_2$/phospho-p53$^{392}$/Ab$_1$-MB/SPCE (curve d) increased significantly. It was not

surprising that the achieved amplification of signal was ascribed to the more amounts of enzymes introduced on the electrode compared with the traditionally labeled HRP-$Ab_2$.

*3.5. Optimization of Detection Conditions*

The incubation time is an important factor for both capturing phospho-$p53^{392}$ antigens and specifically recognizing HRP-CNSs-$Ab_2$. With increasing incubation time in phospho-$p53^{392}$ solution, the peak current increased and tended to steady after 50 min surface (curve a in Figure 4A), indicating a thorough capturing of the antigens on the electrode. When incubating with HRP-CNSs-$Ab_2$ in the second step, the current increased and reached a plateau at 50 min (curve b in Figure 4A), which showed saturated binding sites between antigen and detection antibody. Long time incubation could result in a large nonspecific signal. Therefore, the optimal incubation time for the first and second immunoreactions was 50 min, respectively.

Because of the co-immobilization of enzymes and antibodies on the CNSs nanocarrier, the ration of HRP and $Ab_2$ is another important parameter for the immunoassay signal. Figure 4B revealed that the current of immunosensor increased with the increasing ration of HRP and $Ab_2$ and the maximum response was achieved at the ratio of 200/1. The increase of ratio of HRP and $Ab_2$ could increase the total amount of HRP loaded on per CNSs, which was expected to enhance the response during the immunoassay. However, the excessive HRP reduced the binding sites of CNSs with $Ab_2$, which would decrease the immunocoupling efficiency of capturing phospho-$p53^{392}$ antigen and result in a decreased response. Therefore, the ratio of 200/1 (HRP/$Ab_2$) was selected as the optimal condition for preparation of HRP-CNSs-$Ab_2$ conjugate. The BCA protein assay [39] showed the concentration of active HRP in the HRP-CNSs-$Ab_2$ dispersion was 4.07 μg/mL.

*3.6. Electrochemical Detection of phospho-$p53^{392}$*

The proposed immunosensor using HRP-CNSs-$Ab_2$ conjugate in the amplification

approach was challenged with different concentrations of phospho-p53$^{392}$, as shown in Figure 5A. It can be seen that the SWV currents increased with the increase of phospho-p53$^{392}$. The calibration plots showed a good linear relationship between the reduction peak currents and the logarithm of phospho-p53$^{392}$ concentrations over the range of 0.01 to 5 ng/mL (Figure 5B). The fitted linear regression equation was found to be I (μA) = 5.542 + 2.421 lg c (ng/mL), with a linear regression coefficient of 0.9935. The detection limit at a signal-to-noise ratio of 3σ (where σ is the standard deviation of the signal in a blank solution) was 3.3 pg/mL. The phospho-p53$^{392}$ ELLSA kit showed a linear range from 0.05 to 3 ng/mL with the detection limit of 50 pg/mL. The sensitivity of this amplified electrochemical immunosensor is better than that of ELISA. Moreover, the electrochemical detector used in this work is much simpler and lower in cost compared with the instrument used in the ELISA kit.

To investigate the selectivity, the immunosensor was incubated with detection system of 2 ng/mL phospho-p53$^{392}$ and different possible interfering agents such as p53, phospho-p53$^{15}$, phospho-p53$^{46}$. No remarkable change of current was found in comparison to the result obtained in the presence of phospho-p53$^{392}$ only. The results indicated the immunoassay had a very good selectivity.

To evaluate the intra- and inter-assay coefficients of variation (CVs) of immunosensor array, the intra-assay precision of the analytical method was measured for six replicate determinations. The CVs of the intra-assay were 2.6% and 3.8% at 0.02 and 2.0 ng/mL phospho-p53$^{392}$, respectively. Likewise, the inter-assay CVs on six immunosensor were 3.2% and 5.2% at 0.02 and 2 ng/mL phospho-p53$^{392}$, respectively. These results indicated the immunosensor array had acceptable reproducibility. In addition, the biosensor could be stored at 4 °C. No obvious current degradation was observed after one week and 94% of the initial response remained after one month, indicating acceptable stability.

**4. Conclusions**

In summary, we have successfully designed a multi-enzyme labeling CNSs strategy in a signal amplification procedure and demonstrated its use in the ultrasensitive, selective, and accurate quantification of phospho-p53$^{392}$ by electrochemical immunoassay. MBs were used to introduce a large amount of capture antibody and reduce nonspecific adsorption as well as easy separation. Enhanced sensitivity was achieved by using functionalized CNSs as nanocarriers to link enzyme and signal antibody at high ratio. Compared with traditional strategy, such attractive signal amplification showed excellent performance for detection of phosphorylated protein with a wide linear range, low detection limit and acceptable stability, reproducibility and accuracy. We anticipate that this method can be extended for determination of other proteins and provide a promising potential in clinical applications.

**Acknowledgements**

This work was supported by the National Natural Science Foundation of China (21275062) and the Program for New Century Excellent Talents in University (NCET-12-0871). Y.L. would like to acknowledge the support from a WSU start-up grant. We specially thank Dr. Yongsoon Shin in Pacific Northwest National Laboratory for preparation and characterization of the carbon nanospheres (CNSs).

**References**

[1] J. L. Tubbs and J. A. Tainer, *EMBO J.*, 2011, 30, 2099-2100.

[2] K. H. Vousden and C. Prives, *Cell*, 2009, 137, 413-431.

[3] L. J. Ko and C. Prives, *Genes & Development*, 1996, 10, 1054-1072.

[4] Y. Takahashi, Y. Oda, K. Kawaguchi, S. Tamiya, H. Yamamoto, S. Suita, M. Tsuneyoshi, *Mod. Pathol.* 2004, 17, 660-669.

[5] L. Bai and W. G. Zhu, *J. Cancer Mol.*, 2006, 2, 141-153.

[6] C. Dai and W. Gu, *Trends. Mol. Med.* 2010, 16, 528-536.

[7] M. Matsumoto, M. Furihata and Y. Ohtsuki, *Med. Mol. Morphol.*, 2006, 39, 79-87.

[8] H. Lu, Y. Taya, M. Ikeda and A.J. Levine, Proc. Natl. Acad. Sci. USA. 1998, 95, 6399-6402.

[9] J. H. Jeong, H. Nakajima, J. Magae, C. Furukawa, K. Taki, K. Otsuka, M. Tomita, I. Lee, C. H. Kim, H. W. Chang, K. S. Min, K. K. Park, K. K. Park and Y. C. Chang. Ascochlorin activates p53 in a manner distinct from DNA damaging agents, *Int. J. Cancer*, 2009, 124, 2797-2803.

[10] K. A. Gould, C. Nixon and M. J. Tilby, *Mol. Pharmacol.*, 2004, 66, 1301-1309.

[11] E. Jagelská, V. Brázda, S. Pospisilová, B. Vojtesek and E. Palecek, *J. Immunol. Methods*, 2002, 267, 227-235.

[12] G. Weisinger, Y. Tendler and O. Zinder, *Brain. Res. Protoc.*, 2000, 6, 71-79.

[13] S. Piermarini, L. Micheli, N.H. Ammida, G. Palleschi and D. Moscone, *Biosens. Bioelectron.*, 2007, 22, 1434-1440.

[14] B. V. Chikkaveeraiah, A. A. Bhirde, N. Y. Morgan, H. S. Eden and X. Chen, *ACS Nano*, 2012, 6, 6546-6561.

[15] M. S. Wilson and W. Nie, *Anal. Chem.*, 2006, 78, 6476-6483.

[16] P. Norouzi, V.K. Gupta, F. Faridbod, M. Pirali-Hamedani, B. Larijani and M.R. Ganjali,

*Anal. Chem.*, 2011, 83, 1564-1570.

[17] S. Song, Y. Qin, Y. He, Q. Huang, C. Fan, H. Y. Chen, *Chem. Soc. Rev.*, 2010, 39, 4234-4243.

[18] Y. Li, L. Deng, C. Deng, Z. Nie, M. Yang and S. Si, *Talanta*, 2012, 99, 637-642.

[19] N. Li, P. Zhao and D. Astruc, *Angew. Chem. Int. Ed.*, 2014, 53, 1756-1789.

[20] K. Wang, X. He, X. Yang and H. Shi, *Acc. Chem. Res.*, 2013, 46, 1367-1376.

[21] W. Yang, K.R. Ratinac, S.P. Ringer, P. Thordarson, J. J. Gooding and F. Braet, *Angew. Chem. Int. Ed.*, 2010, 49, 2114-2138.

[22] W. Cheung, F. Pontoriero, O. Taratula, A. M. Chen and H. He, *Adv. Drug. Delivery. Rev.*, 2010, 62, 633-649.

[23] H. Nie, S. Liu, R. Yu and J. Jiang, *Angew. Chem. Int. Ed.*, 2009, 48, 9862-9866.

[24] E. K. Hobbie, D. O. Simien, J. A. Fagan, J. Y. Huh, J. Y. Chung, S. D. Hudson, J. Obrzut, J. F. Douglas, and C. M. Stafford, Phys. Rev. Lett., 2010, 104, 125505.

[25] J. Liu, C. Wang, Y. Jiang, Y. Hu, J. Li, S. Yang, Y. Li, R. Yang, W. Tan and C. Z. Huang, *Anal. Chem.*, 2013, 85, 1424-1430.

[26] Y. Tao, Y. Lin, Z. Huang, J. Ren and X. Qu, *Adv. Mater.*, 2013, 25, 2594-2599.

[27] S. Liu, J. Tian, L. Wang and X. Sun, *Carbon*, 2011, 49, 3158-3164.

[28] X. Yu, B. Munge, V. Patel, G. Jensen, A. Bhirde, J. D. Gong, S. N. Kim, J. Gillespie, J.S. Gutkind, F. Papadimitrakopoulos and J. F. Rusling, *J. Am. Chem. Soc.*, 2006, 128, 11199-11205.

[29] R. Malhotra, V. Patel, J. P. Vaque, J. S. Gutkind and J. F. Rusling, *Anal. Chem*., 2010, 82, 3118-3123.

[30] D. Du, L. Wang, Y. Shao, J. Wang, M.H. Engelhard and Y. H. Lin, *Anal. Chem*. 2011, 83, 746-752.

[31] Y. Shin, L. Q. Wang, I. T. Bae, B. W. Arey and G. J. Exarhos, *J. Phys. Chem. C*. 2008,

112, 14236-14240.

[32] C. Yao, Y. Shin, L. Q. Wang, C. F. Windisch, W. D. Samuels, B. W. Arey, C. Wang, W. M. Risen and G. J. Exarhos, *J. Phys. Chem. C.*, 2007, 111, 15141-15145.

[33] D. Du, Z. Zou, Y. Shin, J. Wang, H. Wu, M.H. Engelhard, J. Liu, I. A. Aksay and Y. H. Lin, *Anal. Chem.*, 2010, 82, 2989-2995.

[34] V. Mani, B. V. Chikkaveeraiah, V. Patel, J. S. Gutkind and J. F. Rusling, ACS Nano, 2009, 3, 585-594.

[35] N. Tran, T. J. Webster, *J. Mater. Chem.*, 2010, 20, 8760-8767.

[36] N. D. Berge, K. S. Ro, J. Mao, J. R. Flora, M. A. Chappell and S. Bae, Environ. Sci. Technol., 2011, 45, 5696-5703.

[37] S.J. Son, J. Reichel, B. He, M. Schuchman and S. B. Lee, *J. Am. Chem. Soc.*, 2005, 127, 7316-7317.

[38] J. A. Linderman, J. A. Shizuru, *J. Immunol.*, 2011, 186, 4191-4199.

[39] M. Mével, M; G. Breuzard, J. J. Yaouanc, J. C. Clément, P. Lehn, C. Pichon, P. A. Jaffrès, P. Midoux, *ChemBioChem*, 2008, 9, 1462-1471.

**Figure Captions**

**Scheme 1.** Schematic illustration of the detection principles of (A) multienzyme labeling amplification strategy using HRP-CNSs-$Ab_2$ and (B) traditional strategy using HRP-$Ab_2$ on $Ab_1$-MB/SPCE sensor platforms.

**Figure 1. (A)** TEM image of MBs. (B) Size distribution of MBs. (C) FTIR spectra of carboxyl MBs (a) and $Ab_1$-MBs (b). (D) UV-vis spectra of MBs (a), $Ab_1$-MBs (b) and $Ab_1$ (c).

**Figure 2.** (A) UV-vis spectra of HRP (a), phopho-$p53^{392}Ab_2$ (b) and HRP-CNSs-$Ab_2$ conjugate (c). (B) XPS of $N_{1s}$ in HRP-CNSs-$Ab_2$ conjugate (a) and in CNSs (b).

**Figure 3. (A)** Cyclic voltammograms of $Ab_1$-MB/SPCE in pH 7.4 PBS (a) and $Ab_1$-MB/SPCE (b), HRP-$Ab_2$/phospho-$p53^{392}$/$Ab_1$-MB/SPCE (c), HRP-CNSs-$Ab_2$/phospho-$p53^{392}$/$Ab_1$-MB/SPCE (d) in pH 7.4 PBS containing 25 μM thionine and 4 mM $H_2O_2$. 0.5 ng/ml phospho-$p53^{392}$ was used.

**Figure 4.** (A) Incubation time on current responses by capturing phospho-$p53^{392}$ (a) and recognizing HRP-CNSs-$Ab_2$ (b) in the presence of 0.5 ng/mL phospho-$p53^{392}$. (B) Effects of ratios of HRP and $Ab_2$ on the current responses in the presence of 0.5 ng/mL phospho-$p53^{392}$.

**Figure 5.** (A) SWV responses acquired at HRP-CNSs-$Ab_2$/phospho-$p53^{392}$/$Ab_1$-MB/SPCE after incubation with 0 (a), 0.01(b), 0.02 (c), 0.05 (d), 0.2 (e), 0.5 (f), 2.0 (g), and 5.0 (h) ng/mL phospho-$p53^{392}$ in pH 7.4 PBS containing 25 μM thionine and 4 mM $H_2O_2$. (B) Calibration curves.

**Scheme 1**

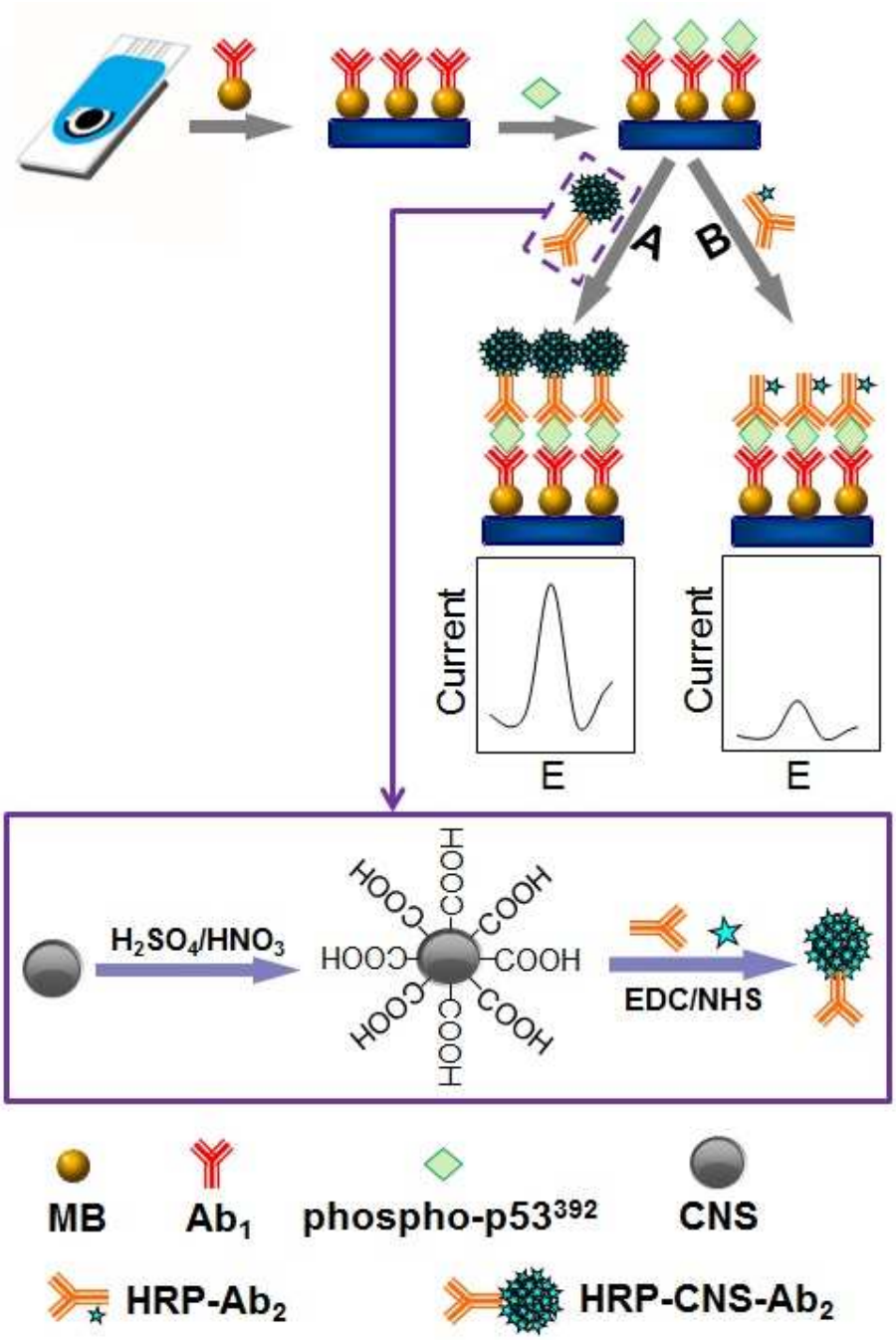

**Figure 1**

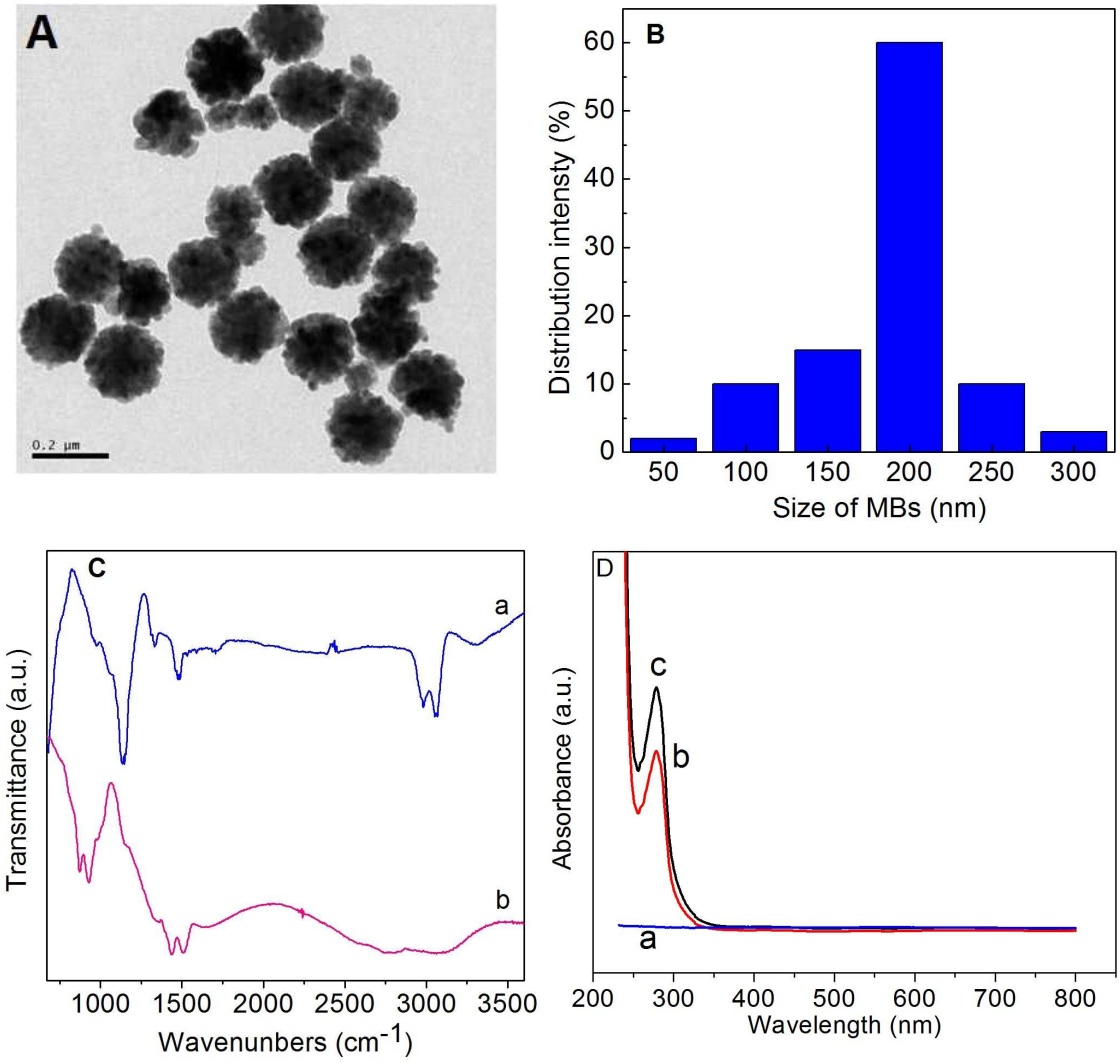

**Figure 2**

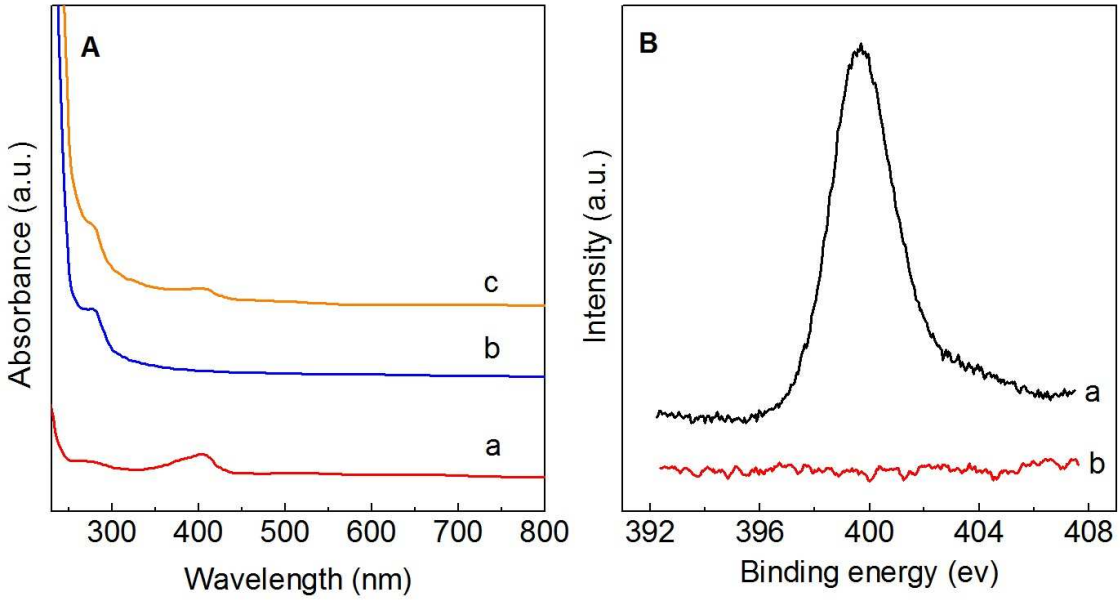

**Figure 3**

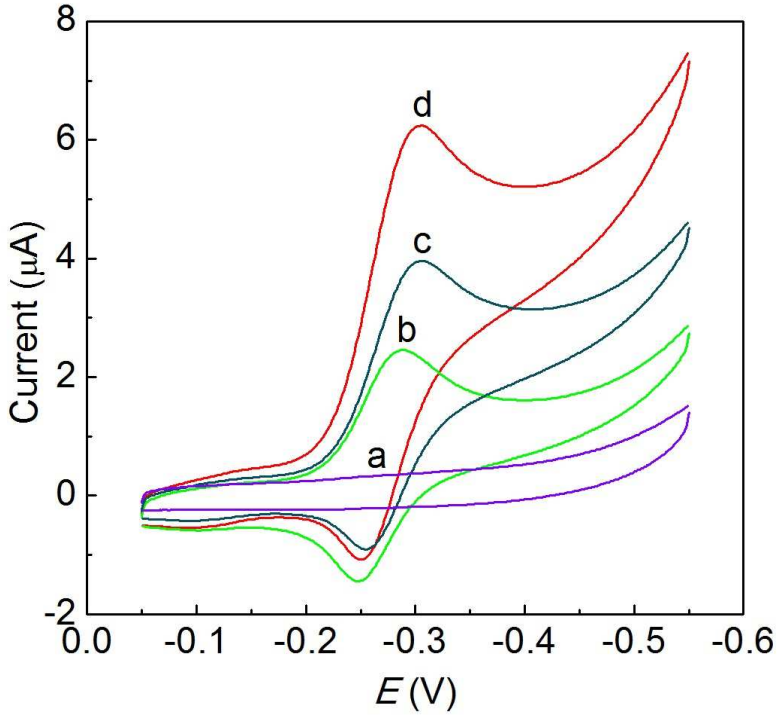

**Figure 4**

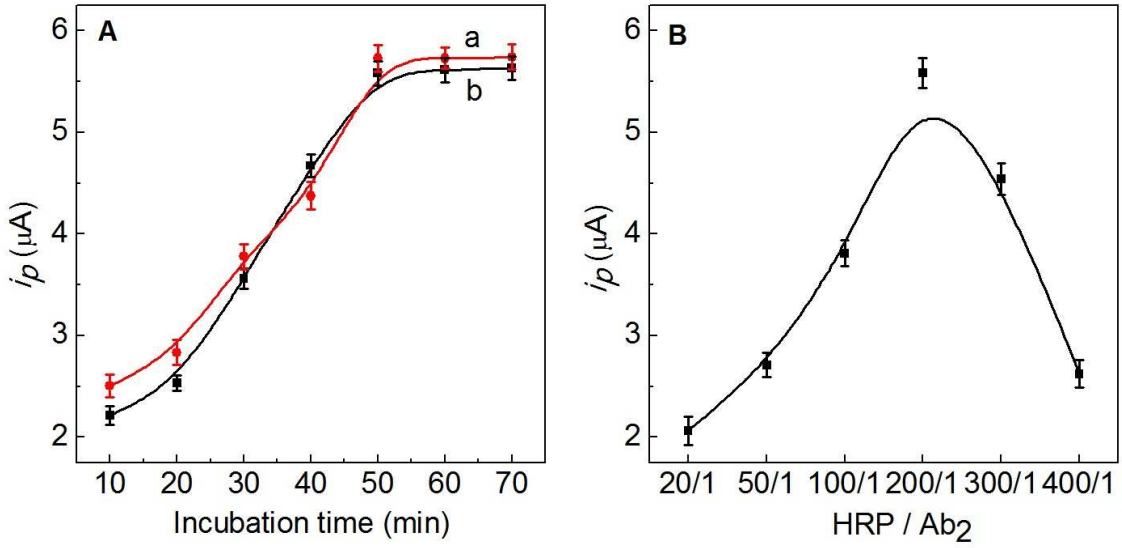

**Figure 5**

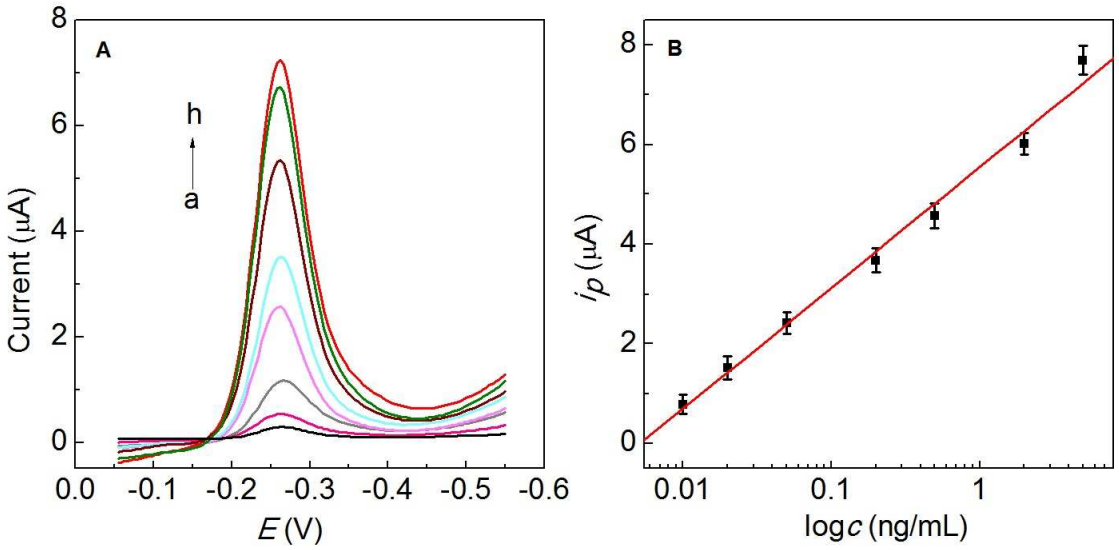

**Table of contents**

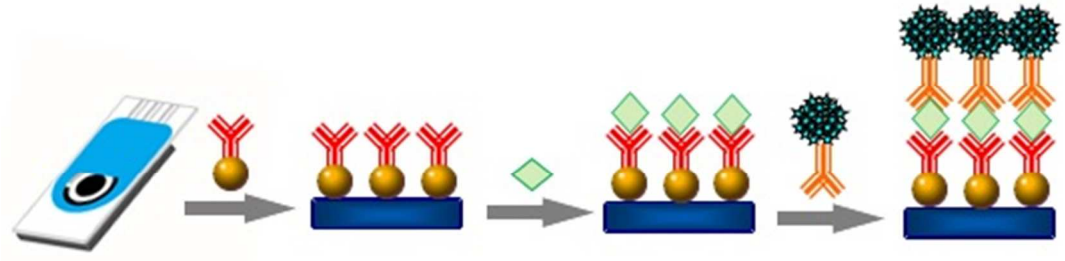

A nanomaterial-based disposable immunosensor was developed for detection of phosphorylated protein using enzyme functionalization of carbon nanospheres as amplification labels.